responsible for another resistivity anomaly found for $\eta\text{-}Mo_4O_{11}$ at 30 K.[9]

No unambiguous evidence for CDW or SDW has been found in $Li_{0.9}Mo_6O_{17}$, so it is not clear whether its resistivity upturn occurring at ~ 25 K is caused by a CDW or an SDW state associated with the Fermi surface nesting. Upon further lowering of the temperature, $Li_{0.9}Mo_6O_{17}$ is found to become a superconductor at 1.9 K.[20] As in the case of CDW and SDW states, a superconducting state also involves orbital mixing (in an indirect manner) between filled and unfilled band levels.[31] Charge carriers of a superconducting state are pairs of electrons having opposite wave vectors, which are described by product functions $\phi(\mathbf{k})\phi(-\mathbf{k})$.[31,34] The driving force leading to superconductivity comes from the interactions (i.e., mixings) of occupied pair functions $\phi(\mathbf{k})\phi(-\mathbf{k})$ with unoccupied pair functions $\phi(\mathbf{k}')\phi(-\mathbf{k}')$, i.e., $\langle\phi(\mathbf{k})\phi(-\mathbf{k})|H'|\phi(\mathbf{k}')\phi(-\mathbf{k}')\rangle$, where the perturbation H' responsible for this mixing is electron–phonon interaction.[34] Depending upon the nature and strength of the perturbations causing orbital mixing, a normal metal with a nested Fermi surface may in principle reach a CDW, an SDW, or a superconducting state upon lowering of the temperature. In most cases, Fermi surface nesting leads to a metal–insulator transition such as CDW or SDW formation. Occurrence of a superconducting state despite the presence of a Fermi surface nesting would mean that the interaction matrix elements $\langle\phi(\mathbf{k})|H'|\phi(\mathbf{k}')\rangle$ responsible for CDW or SDW formation are very small. In cases in which the relative stabilities of CDW, SDW, and superconducting states are similar, preference of one state over the other would

be delicately balanced by a change in temperature and pressure. This appears to be the case for $Li_{0.9}Mo_6O_{17}$. Experimental confirmation of CDW or SDW in $Li_{0.9}Mo_6O_{17}$ would be of interest.

Concluding Remarks

All molybdenum oxide metals contain Mo–O step-layers made up of distorted MoO_6 octahedra, and their unit cells, being large in size and complex in pattern, contain several nonequivalent Mo atoms. Due to the very low d-electron count on Mo in every molybdenum oxide metal, only certain kinds of MoO_6 octahedra contribute their lowest lying t_{2g} levels to form the highest occupied bands responsible for its metallic properties. One can readily recognize such MoO_6 octahedra as the ones whose short Mo–O bonds are long compared with those of other MoO_6 octahedra, because the t_{2g}-block levels are antibonding between Mo and O. Dispersion characteristics of the highest occupied bands are explained by counting in how many Mo–O–Mo bridges the oxygen p orbital can mix between adjacent t_{2g} orbitals at a few special wave vector points. Metals with nested Fermi surfaces, such as the molybdenum oxide metals, are susceptible to a metal–insulator transition leading to a CDW or an SDW state. When CDW and SDW instabilities are weak, a metal may even reach a superconducting state, as in the case of $Li_{0.9}Mo_6O_{17}$. CDW, SDW, and superconducting states are all described in terms of orbital mixing between the occupied and unoccupied levels of a normal metallic state near the Fermi level. What structural factors govern the relative stabilities of CDW, SDW, and superconducting states at low temperatures is an important problem to study.

(34) (a) Bardeen, J.; Cooper, L. N.; Schrieffer, J. R. *Phys. Rev.* 1957, *108*, 1175. (b) Grassie, A. D. C. *The Superconducting State*; Sussex University Press: London, 1975; Chapter 2. (c) Solymar, L.; Walsh, D. *Lectures on the Electrical Properties of Materials*, 4th ed.; Oxford University Press: Oxford, England, 1988; Chapter 14.

A New Two-Parameter Mass Spectrometry

John H. D. Eland

*Physical Chemistry Laboratory, South Parks Road, Oxford, U.K.*

Received May 1, 1989 (Revised Manuscript Received August 9, 1989)

I. Introduction

This Account describes a form of mass spectrometry whose spectra are three-dimensional, showing intensity as a function of two mass parameters. The technique, which is based on charge separation of doubly charged ions, is particularly suitable for the study of fragmentation mechanisms and may eventually find applica-

John H. D. Eland was born in Shropshire, England, on August 6, 1941. He read Chemistry at Oxford under E. J. Bowen and obtained the D.Phil. degree under C. J. Danby. He has since worked in Freiburg with B. Brehm, in Paris with S. Leach, at Argonne with J. Berkowitz, and most recently at Okazaki with K. Kimura. His other research activities include photoelectron spectroscopy and various combinations of electron and ion spectrometries using coincidence techniques, all more or less related to the formation and reactions of molecular ions. His home base is at Oxford, where he is a University Lecturer in Physical Chemistry and a Fellow of Worcester College.

tions in structure determination and analysis.

In regular mass spectrometry, ions created by one of several ionization methods are separated according to their mass-to-charge ratios (m/z) and a spectrum of intensity as a function of m/z is recorded. In the present technique,[1,2] by contrast, the primary process of interest is dissociative double ionization,

$$p + h\nu \rightarrow [p^{2+}] \rightarrow m_1^+ + m_2^+ \; (+m_3)$$
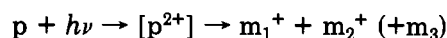
and intensity is recorded as a function of the two m/z values of the ionic products. A photon is shown as the

(1) Eland, J. H. D.; Wort, F. S.; Royds, R. N. *J. Electron Spectrosc. Relat. Phenom.* 1986, *41*, 297–309.
(2) Frazinski, L. J.; Stankiewicz, M.; Randall, K. J.; Hatherley, P. A.; Codling, K. *J. Phys. B* 1986, *19*, L819–824.

ionizing agent, but any particle of sufficient energy can be used. The experiment registers pairs of ions which are correlated in time because they have been formed simultaneously by dissociation of a doubly charged precursor. Two-parameter forms of mass spectrometry already exist and have greatly increased the analytical power of the technique. In tandem mass spectrometry,[3] ions selected from a primary mass spectrum by one analyzer are analyzed again by a second analyzer after unimolecular, collision-induced or photon-absorption-induced secondary fragmentation. A full two-parameter spectrum can be built up by selecting each primary ion in turn, though this is seldom done. The present technique differs by using only a single analyzer and by subjecting each molecule to only one ionization-dissociation event, but nevertheless always gives complete two-parameter spectra.

Ionizing particles that are energetic enough to cause double ionization create doubly charged ions with a wide range of internal energies. Most of the ions will be electronically or vibrationally excited at the moment of formation, and their subsequent fates depend strongly on the amount of internal energy they contain. Many dications have at least one state in which they remain undissociated for the few microseconds needed to pass through a mass analyzer. Such "stable" dications have been known and have been studied intermittently since the earliest years of mass spectroscopy.[4,5] A second group is made up of doubly charged ions that are unstable themselves, but eject neutral particles leaving long-lived doubly charged fragments; these have been extensively investigated since the "E/2E" technique for separating their spectra from those of singly charged ions was invented.[6,7] The third and largest category contains the dications studied by the present technique which undergo charge separation into singly charged fragments. Their existence has been known for many years, since high-kinetic-energy ions in normal mass spectra were attributed to charge separation.[8] A small minority of them undergo charge separation on a microsecond time scale, and as they can be seen as "metastable" peaks in normal mass spectrometers, these have also been studied intensively.[9,10] Most charge-separation reactions take place on a picosecond or nanosecond time scale, however, and escaped detailed observation until the inception of the ion–ion coincidence technique PIPICO (photoion–photoion coincidence).[11,12] PIPICO is the precursor of the present technique, but as a single-parameter method of low mass resolution, it is applicable only to rather small molecules.
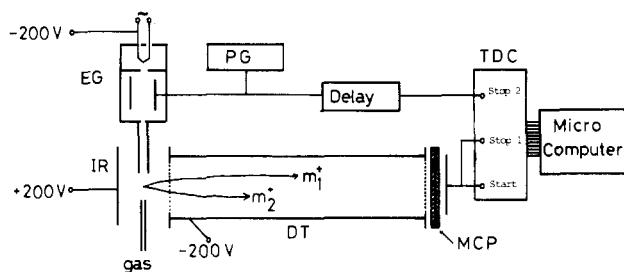
(3) Johnson, J. W.; Yost, R. A. *Anal. Chem.* **1985**, *57*, 758A–768A.
(4) Tate, J. T.; Smith, P. T.; Vaughan, A. L. *Phys. Rev.* **1935**, *48*, 525–531.
(5) Mark, T. D. In *Electron Impact Ionization*; Mark, T. D., Dunn, G. H., Eds.; Springer: Wien, 1985; pp 137–197.
(6) Beynon, J. H.; Mathias, A.; Williams, A. E. *Org. Mass Spectrom.* **1971**, *5*, 303–310.
(7) Mathur, B. P.; Burgess, E. M.; Bostwick, D. E.; Moran, T. F. *Org. Mass Spectrom.* **1981**, *16*, 92–100.
(8) Hustrulid, A.; Kusch, P.; Tate, J. T. *Phys. Rev.* **1937**, *52*, 843–854.
(9) Ast, T. In *Advances in Mass Spectrometry*; Quayle, A., Ed.; Heyden: London, 1980; Vol. 8, pp 555–572.
(10) Ast, T.; Kralj, B.; Kramer, W.; Zigon, D. *Int. J. Mass Spectrom. Ion Processes* **1988**, *86*, 329–339.
(11) Dujardin, G.; Leach, S.; Dutuit, O.; Guyon, P. M.; Richard-Viard, M. *Chem. Phys.* **1984**, *88*, 339–353.
(12) Curtis, P. M.; Eland, J. H. D. *Int. J. Mass Spectrom. Ion Processes* **1985**, *63*, 241–264.

Figure 1. Simplified scheme of one form of apparatus for CSMS. A pulse generator (PG) releases 5-ns bursts of electrons from the electron gun (EG) to ionize gas molecules within the strong field between the ion repeller (IR) and the drift tube (DT). Anode pulses from the multichannel plate ion detector (MCP) are fed as both the start and one stop input to a two-channel time-to-digital converter (TDC), with delayed electron pulses as the second stop. A microcomputer saves the timing data if two ions arrive within a preset time.

The two-parameter form of mass spectrometry developed from PIPICO was originally given the acronym PEPIPICO for photoelectron–photoion–photoion coincidence,[1] but as we now realize that the method is not limited to photon impact, a more general acronym is appropriate. Of various alternatives, CSMS (charge-separation mass spectrometry) seems to be the most informative and is adopted here. The purpose of this Account is to introduce the new technique and illustrate its present capabilities, and to allow potential users to evaluate its possible usefulness for their own applications.

II. Experimental Technique

CSMS can be done in any time-of-flight mass spectrometer with a suitable ionization source and detection electronics; one possible form of apparatus is outlined in Figure 1. The ions that constitute true pairs are identified by the delay between their arrivals at the detector. For any two ions m_1^+ and m_2^+, the times of flight are just $km_1^{1/2}$ and $km_2^{1/2}$ where k is the apparatus constant. If the two ions were born simultaneously by charge separation of a doubly charged precursor, the *difference* of their arrival times will also have the well-defined value $k(m_2^{1/2} - m_1^{1/2})$, whereas for unrelated ions the difference will be random.

To determine the individual flight times, and thus the individual masses, the time of ion formation must be known, and it can be determined in several ways. First, if ionization and ion extraction are continuous, the slow electrons ejected in double ionization by either photons or fast electrons can be detected by an electron multiplier opposite the ion flight tube. This is the approach used in the first instruments; its disadvantage is the limited efficiency of electron detection. Higher count rates are obtained if the ionizing radiation can be provided in pulses short enough not to reduce the mass resolution. A pulsed electron beam is probably the best source for general use, and suitably fast electron guns have been developed for experiments on fluorescence lifetime measurement.[13-15] Electrons can be transported into the ionization zone through a hollow needle to avoid deflection in the ion extraction field of several hundreds of volts per centimeter.

(13) Sutton, J. F. *Rev. Sci. Instrum.* **1972**, *43*, 810–811.
(14) Erman, P.; Brzozowski, J. *Physica Scripta* **1975**, *12*, 177–185.
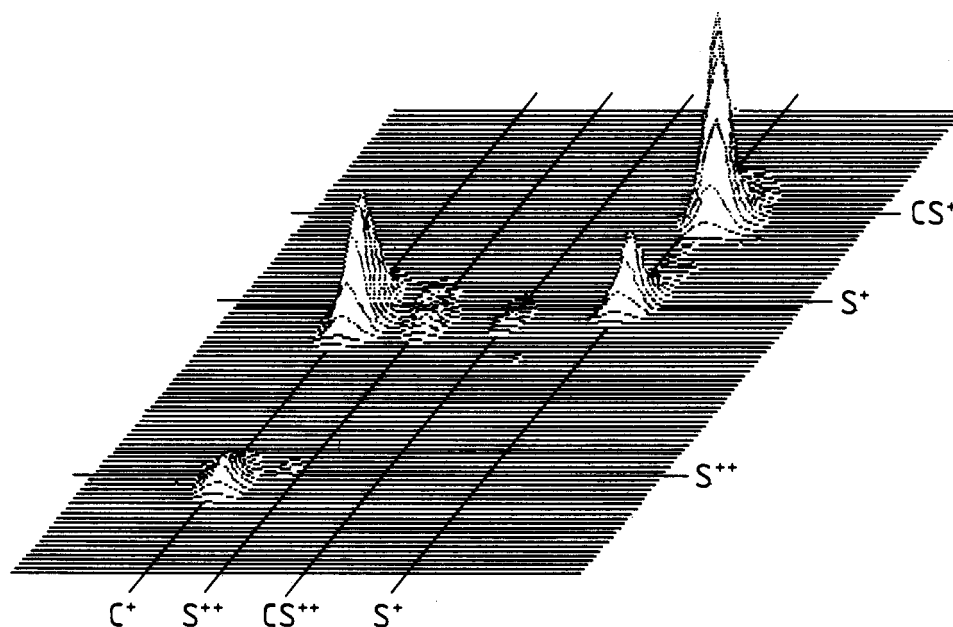(15) Klose, J. Z. *Phys. Rev.* **1966**, *141*, 181–186.

Figure 2. Charge-separation mass spectrum of CS_2 ionized by 1500-eV electrons. Signal intensity is shown on an arbitrary scale as a function of the times of flight of the two ions in each pair. Peaks for equal mass pairs such as $S^+ + S^+$ are cut in half at the $m_1 = m_2$ diagonal, and only the upper half is seen. Weak peaks due to triple and quadruple ionization are also visible.

The time-of-flight mass separator may consist of a simple two-field flight tube,[16] as in the prototype,[1] or of one of the new high-resolution designs.[17-19] The electronic system starts with fast amplifiers and discriminators to provide precise timing of the ion signals and requires two channels of time-to-digital (or time-to-amplitude) conversion interfaced to a computer for rapid readout and processing. One channel measures the delay between ion signals while the other registers the time of flight of the first ion measured from the moment of ionization. The two times are stored in the computer memory only if the delay between ions is in the range expected for correlated pairs. Although complete electronics packages for this purpose cannot be bought "off the shelf", all the components are standard units developed for nuclear and high-energy physics. Computer programs to oversee data gathering and to analyze the data are also an essential part of the technique.

III. Peak Positions and Intensities

Figure 2 shows the charge-separation mass spectrum of carbon disulfide, CS_2, ionized by 1.5-keV electrons[20] just as it comes from the prototype instrument. It illustrates three major features of the spectra, namely, that peaks are seen in one diagonal sector, that the peaks have structure, and that the ion masses making up the peaks only sometimes add up to the intact molecular mass. The peaks are the true coincidence signals from correlated ion pairs, whereas false coincidences, which arise from uncorrelated ions arriving by chance with time delays in the range expected for true pairs, would form ridges at the masses of abundant ions in the

normal mass spectrum. The peaks are above the diagonal because the first ion to arrive fixes the position on one axis and the second ion, which fixes the other coordinate, always arrives later. The structure of the peaks is a result of the energy release on charge separation and is explained in section IV. Finally, pairs of ion masses add up to a sum less than the parent mass in all *three-body* reactions where neutral fragments are formed in addition to the two ions. Neutrals may be ejected either before or after charge separation, in overall mechanisms referred to as *deferred charge separation* and *secondary dissociation*, respectively.

In deferred charge separation, the reaction sequence is

$$m^{2+} \rightarrow m_1^{2+} + m_2$$

$$m_1^{2+} \rightarrow m_3^+ + m_4^+$$
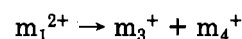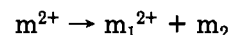
In secondary dissociation, the reactions are

$$m^{2+} \rightarrow m_1^+ + m_2^+$$

$$m_1^+ \rightarrow m_3^+ + m_4$$
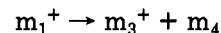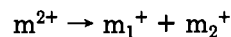
Combinations of these two sequences can also occur, and a third mechanism for three-body reactions, simultaneous coulomb explosions where all the fragments separate at once, is also possible. Present results suggest that simultaneous coulomb explosion of polyatomic dications is rather rare, however, at least at energies below inner shell ionization thresholds.

Triatomic and Small Inorganic Molecules. The first molecules subjected to CSMS were triatomics and related small molecules; studies of CS_2,[22] OCS,[22] NO_2,[23] SO_2,[22] N_2O,[24] SF_6,[2] and NH_3[25] have appeared. The

(16) Wiley, W. C.; McLaren, I. H. *Rev. Sci. Instrum.* **1955**, *26*, 1150–1157.

(17) Yefchak, G. E.; Enke, C. G.; Holland, J. F. *Int. J. Mass Spectrom. Ion Processes* **1989**, *87*, 313–330.

(18) Brunee, C. *Int. J. Mass Spectrom. Ion Processes* **1987**, *76*, 125–237.

(19) Sakurai, T.; Fujita, Y.; Matsuo, T.; Matsuda, H. *Int. J. Mass Spectrom. Ion Processes* **1985**, *66*, 283–290.

(20) Hagan, D. A.; Eland, J. H. D. *Rapid Commun. Mass Spectrom.* **1989**, *6*, 186–189.

(21) Eland, J. H. D.; Coles, L. A.; Bountra, H. *Int. J. Mass Spectrom. Ion Processes* **1989**, *89*, 265–285.

(22) Eland, J. H. D. *Mol. Phys.* **1987**, *61*, 725–745.

(23) Fournier, P. G.; Eland, J. H. D.; Millie, P.; Svensson, S.; Price, S. D.; Fournier, J.; Comtet, G.; Wannberg, B.; Karlsson, L.; Baltzer, P.; Kaddouri, A.; Gelius, U. *J. Chem. Phys.* **1988**, *89*, 3553–3564.

(24) Price, S. D.; Eland, J. H. D.; Fournier, P. G.; Fournier, J.; Millie, P. *J. Chem. Phys.* **1988**, *88*, 1511–1515.
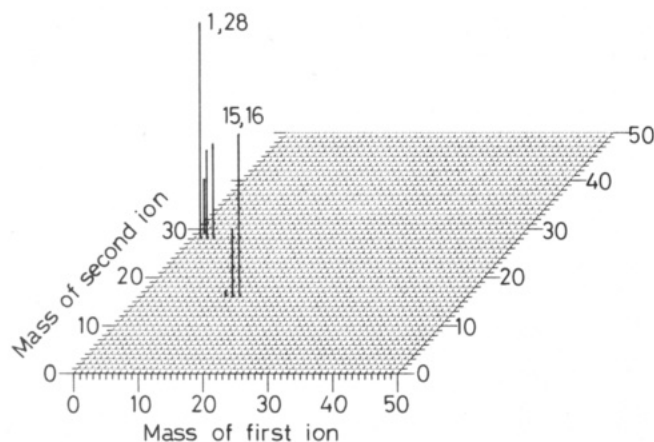
Figure 3. Charge-separation mass spectrum of methylamine ionized by 30.4-nm (40.8-eV) light.

Figure 4. Charge-separation mass spectrum of perfluorocyclobutane at 30.4 nm.

spectra are simple, but illustrate some general observations. First, in competition between simple bond cleavages, low-energy products usually seem to be formed in preference to more energy costly ones; for instance, $NO^+ + N^+$ pairs are more abundant than $N_2^+ + O^+$ pairs from N_2O, and $CO^+ + S^+$ dominate over $CS^+ + O^+$ from OCS. The branching ratios depend on the amount of energy deposited in the molecules; as more energy is made available, higher energy channels, particularly three-body reactions, become more abundant. Many spectra have been taken with He II light of 40.8-eV photon energy where the branching ratios are changing quite rapidly with wavelength; a higher energy would probably be better. Synchrotron radiation work including the CSMS study of NH_3[25] and earlier PIPICO studies have shown that the branching ratios become relatively insensitive to wavelength at around 60 eV; unfortunately no laboratory source of light of this energy is available. With electron-impact ionization, the form of the threshold law[26] suggests that the amount of energy deposited should change only slowly with incident energy. This is borne out by data on electron-impact double ionization,[5] which show that at energies between 100 and 200 eV ion yields are high and variations in branching ratio are rather small. Thus the optimum ionization source for a standard form of CSMS is probably a pulsed electron gun at an energy of 150 or 200 eV.

Secondly, although simple cleavages dominate the charge-separation spectra of triatomics, rearrangement reaction products are also observed. Double ionization of OCS, for instance, yields $C^+ + SO^+$ pairs as well as the abundant $CO^+ + S^+$ and $CS^+ + O^+$, some $S_2^+ + C^+$ is observed from CS_2, and some $O_2^+ + S^+$ is observed from SO_2. The naive expectation, based on the large exothermicities and added impetus of coulomb repulsion, that charge separations would be wholly direct reactions is not correct.

Monosubstituted Methanes. The monofunctional methyl compounds have been studied by CSMS[27] as the first members of homologous series and also as a group for which complete mass separations are possible at low resolution. In contrast to triatomic molecules where the number of possible ion pairs is strictly limited, even for
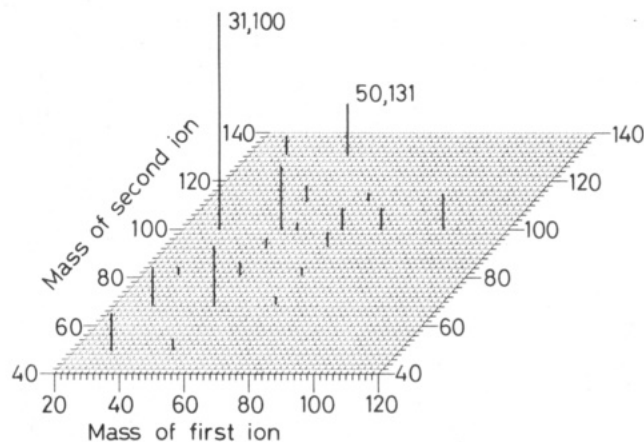
(25) Stankiewicz, M.; Hatherley, P. A.; Frazinski, L. J.; Codling, K. *J. Phys. B* **1989**, *22*, 21–31.
(26) Wannier, G.H. *Phys. Rev.* **1953**, *90*, 817–825.
(27) Ruhl, E.; Leach, S.; Price, S. D.; Eland, J. H. D., in press.

such small species as the monosubstituted methanes the CSMS spectra are quite complex. The presence of diagonally, vertically, and horizontally adjacent peaks in two-parameter spectra makes the raw data look congested even when they are well resolved, so spectra are given here as two-parameter stick diagrams analogous to the familiar form of regular mass spectra. The spectrum of methylamine is shown as an example in Figure 3.

The charge separations of the methyl compound dications can be classified as C–X bond cleavage, where X is the functional group, or H–CX cleavage, both also including various losses of neutral hydrogen. Cleavage of the C–X bond is predominant for CH_3I, CH_3Cl, CH_3SH, and CH_3CHO, the two reactions are of equal abundance for CH_3CN, and C–H cleavage is stronger for CH_3OH and CH_3NH_2. These abundances correlate surprisingly well with the relative C–X and C–H bond strengths in the neutral molecules, since the C–H bond is stronger than C–X in the halides, thiol, and aldehyde, while they are of equal strength, or the C–X bond is stronger, in the alcohol, amine, and cyanide. The CSMS peak shapes (section IV) show that the three-body reactions are mainly secondary dissociations of primary monocations. The C–H cleavage reactions usually start by formation of $H_3^+ + CX^+$; in methylamine and methanol, substantial numbers of H_3^+ ions are detected as members of pairs, while in other cases most of the primary H_3^+ ions dissociate further. Three-body reactions involving C–X cleavage similarly start by simple C–X bond breakage on charge separation, followed by secondary dissociation of the CH_3^+ primary ions. A remarkable contrast between three-body and two-body reactions appears for CH_3OD, where three-body charge separations seem to involve complete H-atom scrambling, while the two-body reactions show almost complete label retention.

Perfluoro Aliphatic Compounds. The most notable change on going from the methyl compounds to the larger perfluoro compounds, and also on increasing size of molecules within this group, is that the proportion of two-body reactions diminishes very rapidly. This is noticeable in the CSMS spectrum of perfluorocyclobutane in Figure 4 and is shown even more clearly by the *pair-sum* or *apparent-precursor* spectrum of the same compound in Figure 5. This spectrum gives intensity as a function of the sum of the masses, $m_1 + m_2$, for ions observed in pairs. It is derived
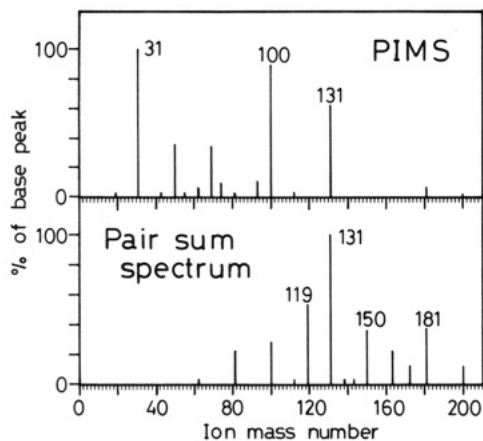
Figure 5. Pair-sum spectrum showing apparent doubly charged precursors of charge-separation products from perfluorocyclobutane ionized by 30.4-nm light (below) and the photoionization mass spectrum (above) for comparison. Note the concentration on high masses and strong parent ion (mass 200) in the precursor spectrum.
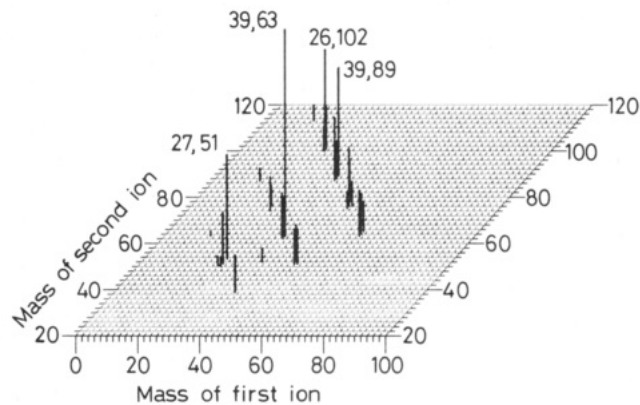

Figure 6. Charge-separation mass spectrum of naphthalene at 30.4 nm. Perdeuterionaphthalene was used to ensure complete mass separations, but the equivalent spectrum for normal naphthalene is shown here. Isotope effects are very small.

by adding up intensity in the CSMS spectrum along the diagonal lines on which $m_1 + m_2$ is constant and therefore shows abundances of doubly charged ions from which the ion pairs could have originated. Because of secondary dissociations, however, many observed ion pairs are not the primary products of charge separation, and the spectrum is one of *apparent* rather than true precursors. The normal photoionization mass spectrum is given in the upper part of the figure for comparison.

The pair-sum spectrum shows the tendency of perfluorocyclobutane dications to fall apart in three-body reactions, but it has a much greater emphasis on high masses, including parent ions, than the normal mass spectrum; the average mass is almost a factor of 2 higher. As a single-parameter representation of the results of CSMS, this sort of spectrum is extremely useful. The masses are high and likely to be structurally significant, and for every peak, the full CSMS data contain at least one pair of fragments of which the precursor is composed. The parent ion (mass 200) in the pair-sum spectrum of C_4F_8, for instance, is made from the pair (100,100) only, but the next higher mass peak at 181 is made up from three pairs of ions, (50,131), (69,112), and (81,100).

Examination of the CSMS peak shapes (section IV) shows that most of the larger perfluoro dications dissociate in three steps: first, by loss of a neutral entity, usually an F atom; secondly, by charge separation; and thirdly, by dissociation of one of the singly charged ions so produced. In perfluorocyclobutane, for instance, only 10% of pairs come from two-body reactions, and 85% of primary singly charged ions undergo secondary fragmentation. The fraction of two-body reactions becomes even smaller for larger species, a tendency that can be rationalized by a simple energy model.

Double ionization requires a minimum energy transfer into the molecule of $2.8I$, where I is the first ionization potential.[28] The minimum energy needed for cation pair formation is the sum of a bond dissociation energy D and two radical ionization potentials I' and I''. From estimates of these quantities for the

perfluoro compounds ($I = 12$ eV, $D = 4$ eV, $I' = I'' = 10$ eV), we find that even the minimum energy transfer in double ionization leaves about 10 eV excess energy available above the pair formation threshold. As molecular size increases, a decreasing part of this energy is released as coulomb repulsion; if 2 eV is released, for instance, more than enough energy is left to rupture another bond. If 8 eV is divided equally between two fragments, both may just remain stable, but if one fragment gets most of the energy, it will inevitably dissociate. According to the statistical model,[29] an equal division is likely only if the fragments are of equal size; this explains why in all the large perfluoro compounds the heaviest precursors are made up of two heavy fragments, never one light ion and one heavy one.

Aromatic Molecules. The excess-energy model implies that aromatic compounds, which have low ionization potentials and must break several bonds in order to separate into any fragment pair, should be stable as doubly charged ions. The excess energy after charge separation will be small or zero unless double ionization deposits more than the minimum energy in the molecule, so secondary fragmentation should not be common. This prediction is well supported by the observations.

In the CSMS spectrum of benzene,[30] all significant charge separations stem from doubly charged precursors which retain a full C_6 skeleton, only H atoms being lost as neutrals. For naphthalene,[31] Figure 6, the strongest groups of peaks lie on a diagonal that represents $C_{10}H_n^{2+}$ precursors, but subsidiary diagonals corresponding to C_8 and C_6 precursors are also evident. The precursor spectra of azulene and quinoline[32] likewise have peaks for even heavy atom numbers only. For benzofuran and benzothiophene, however, which have nine heavy atoms, the precursor spectra contain strong peaks only for odd heavy atom numbers. This contrast means that the stability of the neutral fragment, predominantly C_2H_2, determines the precursor spectrum. If the stability of the ionic products were the determining factor, precursors with even numbers of heavy atoms would be seen again. The peak shapes indicate that the ejection of neutral C_2 fragments occurs as a first

(28) Tsai, B. P.; Eland, J. H. D. *Int. J. Mass Spectrom. Ion Phys.* **1980**, *36*, 143–165.

(29) Wallenstein, M. B.; Krauss, M. *J. Chem. Phys.* **1961**, *34*, 929–936.
(30) Richardson, P. J.; Eland, J. H. D.; Lablanquie, P. *Org. Mass Spectrom.* **1986**, *21*, 289–294.
(31) Leach, S.; Eland, J. H. D.; Price, S. D. *J. Phys. Chem.*, in press.
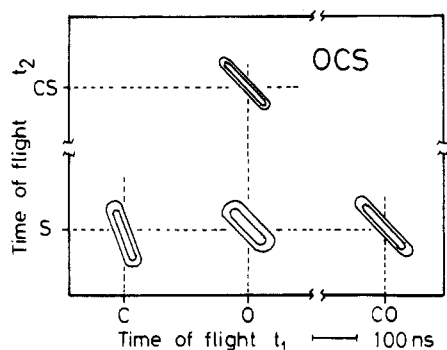(32) Leach, S.; Eland, J. H. D.; Price, S. D. *J. Phys. Chem.*, in press.

Figure 7. Simplified contour diagrams showing the main features of the CSMS peak shapes for the four main ion pairs from OCS ionized by 30.4-nm light. The contours are drawn at two-thirds and one-third of the maximum intensity in each peak.

step in the doubly charged ion breakdown, so the predominant mechanism is deferred charge separation.

## IV. Peak Shapes and Reaction Mechanisms

Pathways and Kinetic Energy Releases. When CSMS spectra are drawn on an expanded scale, each peak is found to have an individual shape.[22] The shapes can be seen in projections like Figure 2 or, more clearly, in contour diagrams such as Figure 7. Most peaks are elongated ovals or ellipses with characteristic length, width, and slope, the slope being the inclination of the long axis of the peak to the coordinate system. Time rather than mass coordinates are appropriate here because initial ion velocities, which produce the peak shapes, are linearly related to deviations of ions' arrival times from their nominal values.

The *lengths* of CSMS peaks are determined by kinetic energies released in the charge separation step, just like the widths of peaks in PIPICO or the widths of metastable peaks in mass spectrometry. The length of the peak for $CO^+ + S^+$ from OCS in Figure 7, for instance, indicates a release of 5.3 eV, which would correspond on a coulomb repulsion model to an intercharge distance of 0.27 nm before charge separation. The interpretation of energy releases in terms of intercharge distances, although naive, can be helpful in analyzing mechanisms. In the CSMS spectrum of methanol, for instance, the products $CH_3^+ + OH^+$ seem to originate at an intercharge distance of 0.22 nm in the dication. The products $CH_2^+ + OH_2^+$, on the other hand, seem to be released from a longer distance of about 0.3 nm, consistent with an ab initio calculation[33] of the bond lengths in the ylide dication $[CH_2OH_2]^{2+}$ to which the methanol dication may rearrange. The special feature of CSMS is that it gives energy releases like these for every peak in the spectrum.

The *widths* of CSMS peaks are related to kinetic energies released in steps other than the charge separation itself. For two-body reactions, such as the formation of $CO^+ + S^+$ and $CS^+ + O^+$ from OCS in Figure 7, the width arises from the thermal velocities of the molecules (Maxwell–Boltzmann distribution) before ionization. If ejection of a neutral fragment occurs before charge separation (deferred charge separation mechanism) or afterward (secondary dissociation), energy release in either of these steps will broaden the peak. The peak for $S^+ + O^+$ from OCS in Figure 7 is

(33) Yates, B. F.; Bouma, W. J.; Radom, L. *J. Am. Chem. Soc.* **1986**, *108*, 6545–6554.

of this type, but the exact mechanism is not clear in this case.

The *slope* of a CSMS peak is the most important clue to the reaction mechanism. For all two-body reactions, the slope is exactly −1 and the peaks are diagonal; this is also true of deferred charge separations. If secondary dissociation occurs, however, the absolute value of the slope is usually just the ratio of the mass of the product ion to the mass of its precursor. Slopes both larger and smaller than −1 are found, depending on whether the secondary product ion is the lighter or heavier member of the final ion pair. Measurements of these slopes, which can be made very accurately for intense peaks, allow the pathways of secondary dissociation reactions to be deduced; this is the source of the information on mechanisms of various pair formation reactions discussed in the last section. For the ion pair $C^+ + S^+$ from OCS in Figure 7, the slope is very close to the ratio −28/12, showing that the mechanism is

$$OCS^{2+} \rightarrow CO^+ + S^+$$
$$CO^+ \rightarrow C^+ + O$$
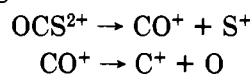
The reason for this very convenient property of CSMS peak slopes is that in time-of-flight mass spectra the deviation of an ion's arrival time from the nominal value is directly proportional to its initial momentum along the spectrometer axis. When a doubly charged ion breaks into just two monocations, the two must have equal and opposite initial momenta to conserve linear momentum. This produces anticorrelation in the arrival-time deviations of the two ions, and the slope of −1. If one of the primary ions dissociates later without any energy release, its velocity stays the same and its momentum changes by the mass ratio. If the primary ion has time to rotate freely before it dissociates, any new energy release will only broaden the peak.

Reaction Times. For a sharp peak in the CSMS spectrum, a pair of ions must be formed in the source within less than 100 ns of the initial ionization. Slower reactions, taking between about 100 and 5000 ns, give rise to "metastable" signatures in the two-parameter spectra. If initial charge separation is slow, a weak line is seen connecting the pair peak with a point on the diagonal where the doubly charged precursor would arrive.[1] If charge separation is fast but secondary decay is slow, a ridge is found connecting the primary and secondary pair peaks. Both these phenomena of slow ionic decay represent a small minority of ions. A novel feature of CSMS is that it provides a window on fast secondary decays with a time scale of 10 fs to 10 ps where conventional rate measurements are extremely difficult.

The slope of an ion pair peak from a secondary dissociation mechanism is expected to be just the mass ratio, as explained above, identifying the reaction pathway. In fact, the slope has this exact value only if the two primary ions have escaped the zone of coulomb repulsion before secondary fragmentation. For an energy release of 3 eV, ions of mass 50 will reach a separation of 10 nm in 8 ps. At the other extreme, the observed slope will be indistinguishable from −1 if secondary dissociation takes place before significant release of the primary coulomb repulsion energy, in a time of the order of 10 fs. Between these two extremes, the slope of the peak must lie between the nominal mass ratio and −1; from its value, the reaction lifetime

can be worked out, if the pathway is known or assumed. This is possible mainly for small molecules where there are few available pathways and reactions tend to be fast enough to fall in the measurable range. For larger molecules with many reaction pathways, the secondary reactions tend to be slow, giving slopes close to simple mass ratios.

In methyl iodide, for instance, the peak slopes for the reactions leading to $CH_2^+ + I^+$, $CH^+ + I^+$, $C^+ + I^+$, and $H^+ + I^+$ are all slightly smaller than the mass ratios for production of the lighter fragments by decay of methyl ions. All four deviations are explained if CH_3^+ first separates from I^+ to a distance of about 1 nm and then breaks down into the various final products. The reaction time is approximately 300 fs. Similar deductions can be made on the secondary decay of H_3^+ from charge separations in the methyl compound dications, where lifetimes of the order of 20 fs are found.[25] Alternative interpretations involving directed secondary energy releases would be possible, but the fast reaction interpretation is more natural and is supported by the agreement between times for different reactions and for different isotopic species.

V. Concluding Remarks

Charge-separation mass spectrometry is an absolutely new technique, being used at present by just three groups worldwide. The experiments are not yet routine in any laboratory, and it generally takes several hours to gather a spectrum; this situation may soon improve as no fundamental difficulties are involved. The emphasis hitherto has been on the formation and stability of doubly charged ions, and extensions to triple and higher multiple ionization are already being investigated, but the characteristics of the technique, described in this Account, should make it more widely useful than just a tool for the study of highly charged ions. For instance, the pair-sum spectra, and presumably the equivalent spectra from higher multiple ionization, emphasize high masses, including parent ions even though high-energy radiation is used. Reference to the full CSMS spectra then gives a fragmentation pattern for each high-mass species. This suggests applications similar to those of "soft" ionization methods in characterization of large or delicate molecules, such as biopolymers or van der Waals clusters in molecular beams. The mechanistic information available from peak shapes in the spectra is unparalleled, including the identity of neutral species, kinetic energy releases, and sometimes reaction rates. Peak shapes in CSMS should be an important complement to metastable peaks in conventional mass spectra as a probe of singly charged ion fragmentations, because they refer to fast, majority reaction processes rather than to a possibly unrepresentative minority of slow reactions. Applications to analysis are speculative at present and must await the technical developments, now in progress, toward higher mass resolution, greater sensitivity, and the study of nonvolatile samples.

Concerted Mechanisms of Acyl Group Transfer Reactions in Solution

Andrew Williams

University Chemical Laboratories, Canterbury, England CT2 7NH

Received January 23, 1989 (Revised Manuscript Received June 22, 1989)

This Account describes recent studies of acyl group transfer reactions in aqueous solution using polar substituent effects in systems where it is possible to discriminate between concerted and nonconcerted mechanisms. Distinction between concerted and stepwise mechanisms is a major problem in chemistry because there are few reactions involving a single bond change; this importance is amply recognized by the attention devoted to the subject. The most celebrated discussions of concertedness refer to pericyclic reactions,[1] base-catalyzed elimination,[2a] and nucleophilic aliphatic substitution reactions.[2b] It is conceptually impossible to demonstrate a concerted mechanism which may be defined as a process with a single transition state;[3]

Andrew Williams has been the subject of a previous biographical note in this journal (*Acc. Chem. Res.* 1984, *17*, 425). Since that time he has become Chairman of the Chemistry Department at the University of Kent.

Scheme I
Stepwise Mechanisms for the Transfer of the Acyl Group (A) between Nucleophiles (L⁻ and Nu⁻)
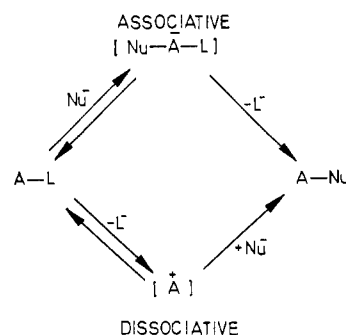
nonconcerted mechanisms can be demonstrated by the observation or inference of the existence of an inter-